

High Accuracy Satellite Drag Model (HASDM)

Mark F. Storz^{*}, Bruce R. Bowman^{*} and Major James I. Branson[†]

Abstract

The dominant error source in force models used to predict low perigee satellite trajectories is atmospheric drag. Upper atmospheric density models do not adequately account for dynamic changes in neutral density leading to significant errors in predicted satellite positions. The Air Force Space Battlelab's High Accuracy Satellite Drag Model (HASDM) estimates and predicts (out three days) a dynamically varying global density field. HASDM includes the Dynamic Calibration Atmosphere (DCA) algorithm that solves for the phases and amplitudes of the diurnal and semidiurnal variations of upper atmospheric density near real-time from the observed drag effects on low-perigee inactive payloads and debris. The density correction is expressed as a function of latitude, local solar time and altitude. In HASDM, a time series filter predicts the DCA density correction parameters as a function of predicted extreme ultraviolet (EUV) energy index $E_{10.7}$ and predicted geomagnetic storm index a_p and as a function of the recent (last 27 days) time series of the density correction parameters. The $E_{10.7}$ index is generated by the SOLAR2000 model, the first full spectrum model of solar irradiance. The estimated and predicted density fields will be used operationally to significantly improve the accuracy of predicted trajectories for all low perigee satellites.

Introduction

The High Accuracy Satellite Drag Model is an initiative launched by the Air Force Space Battlelab in January 2001 to improve Air Force Space Command's ability to meet the stringent Space Surveillance Capstone Requirements for satellite trajectory prediction accuracy. For low perigee satellites (<600 km altitude), these requirements are not consistently met, largely because current atmospheric density models have errors of 15% to 20%^{8,9}. This can affect missions like maneuver planning, re-entry predictions, collision avoidance, risk analysis, and acquiring

satellites with narrow field-of-view sensors. The Space Battlelab funded this initiative because of the substantial payback expected, and the fact that it involves more risk than the acquisition community or operational community are willing to fund. It is also well suited to the Space Battlelab's project criteria of demonstrating unconventional ways of using existing data and technology to meet mission requirements, and being able to demonstrate this in 18 months or less. This initiative leverages off an earlier Space Battlelab project¹⁰ that demonstrated the potential of the basic technique, even when only one satellite is used to extract the drag effects.

This initiative optimizes the earlier approach by simultaneously processing drag information from the trajectories of 75 inactive payloads and debris (*calibration satellites*) to solve for a dynamically changing global correction to the thermospheric and exospheric density. The thermosphere is the layer of the atmosphere from 90 km to ~600 km altitude. The exosphere is the layer above the thermosphere. Unlike the earlier effort, that used derived quantities from the orbit determination process, this initiative involves the direct processing of satellite tracking observations from the Space Surveillance Network. It determines the thermospheric density correction parameters, while solving for the states of the calibration satellites, in a single estimation process, known as the Dynamic Calibration Atmosphere (DCA). The density corrections reflect dynamic changes in the diurnal and semidiurnal variations³.

The initiative also capitalizes on the new SOLAR2000 model developed for the Space Environment Center by Space Environment Technologies, Inc.¹⁵ This is the first-ever full solar spectrum model and acts like a data fusion engine, assimilating many different sources of solar irradiance data. It can generate many products related to the sun's electromagnetic radiation output. However, this initiative makes use of the extreme ultraviolet (EUV) band of radiation. This radiation is the major heat source in the thermosphere, causing the atmospheric

^{*} Air Force Space Command, Space Analysis Center (ASAC), Peterson AFB, CO 80914-4650

[†] Air Force Space Battlelab, Schriever AFB, CO 80912-7383

density to change up to 2 orders of magnitude, throughout the 11-year solar cycle⁶. SOLAR2000 has recently been modified to produce a 3-day prediction of the EUV radiation in the form of an effective $F_{10.7}$ index based on the intensity of this radiation. This new index is known as $E_{10.7}$, and when input to existing models requiring $F_{10.7}$, automatically boosts their accuracy performance.

This project also includes the development of a prediction model that maps the time series of solar and geomagnetic indices (including $E_{10.7}$) to the density correction parameters estimated by DCA. It also extrapolates information from the time series of the density correction coefficients using Fourier analysis. DCA's high-resolution thermospheric density correction, together with the 3-day index prediction, should significantly improve space control operations.

Background

The goal of this initiative is to estimate an accurate global correction to the modeled thermospheric neutral density using drag effect information from the trajectories of inactive satellites and orbiting debris, known as calibration satellites. The greater the thermospheric density, the faster low-perigee objects spiral inward. Air Force first explored the concept of estimating thermospheric density from satellite trajectories in 1995 at Air Force Space Command and Air Force Research Laboratory using Small Business Innovative Research funds. This led to the earlier Space Battlelab initiative, the Modified Atmospheric Density Model (MADM)¹⁰, completed in March 2000.

In MADM, the main parameter used to determine the density was the estimated ballistic coefficient. In the orbit determination process, this is a solve-for parameter, just like the elements of the satellite's state vector. The ballistic coefficient is a measure of how much the object is affected by atmospheric drag. The larger the ballistic coefficient, the greater affect

the atmosphere has on the object⁷. The true ballistic coefficient B_{true} and the true atmospheric density ρ_{true} , together with the speed V of the satellite, determine the drag acceleration a_D through the following expression:

$$a_D = \frac{1}{2} B_{\text{true}} \rho_{\text{true}} V^2 \quad (1)$$

The true density ρ_{true} is generally not known, so the model density ρ_{model} is used instead. The estimated ballistic coefficient B_{model} , varies depending on the error in the modeled density ρ_{model} . If the model density is low when compared to the real density, then the estimated ballistic coefficient B_{model} is larger than its true value. Conversely, when the model atmospheric density is too high, B_{model} is smaller than its true value. Therefore, information about the bias in the atmospheric model is contained within the values for B_{model} . The "observed" drag acceleration a_D has nearly the same value, regardless of the value of ρ_{model} and B_{model} . Therefore,

$$a_D = \frac{1}{2} B_{\text{model}} \rho_{\text{model}} V^2 \quad (2)$$

This implies that $B_{\text{true}} \rho_{\text{true}} \cong B_{\text{model}} \rho_{\text{model}}$ and that $\rho_{\text{true}} \cong (B_{\text{model}}/B_{\text{true}}) \rho_{\text{model}}$. The ratio $B_{\text{model}}/B_{\text{true}}$ is referred to as the "scaled" estimated ballistic coefficient B_{scale} . Figure 1 shows that Low Earth Orbit (LEO) satellites with different orbits generally exhibit similar trends in their B_{scale} time series¹³. This indicates that B_{scale} can be used to correct the model density globally to obtain a rough estimate of the true density. Once a value for B_{true} is estimated by averaging many successive values of B_{model} , then the value for ρ_{true} may be computed. MADM exploited this information from a single calibration satellite to deduce the bias of the model atmosphere. Since MADM used only one satellite, it produced modest results. It reduced the rms of the fit span error by about 20% and reduced the error growth rate by about 10% for a 1-day prediction. HASDM reduced the rms of the fit span error by about 30% and is also expected to produce better results over a 1-day prediction span².

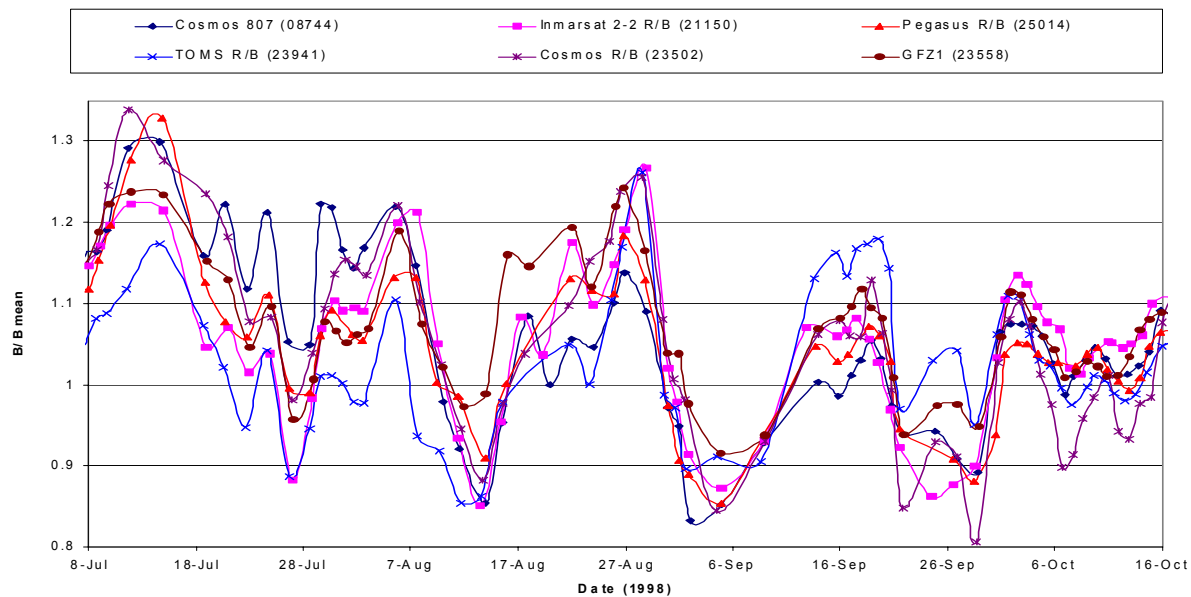


Figure 1. Scaled Ballistic Coefficient Histories ($B_{\text{scale}} = B_{\text{model}} / B_{\text{true}}$)

Dynamic Calibration Atmosphere

MADM employed a separate orbit determination process and a separate density estimation process. In HASDM's Dynamic Calibration Atmosphere (DCA), these two processes are combined into a single estimation process. This is a weighted least squares differential correction across all calibration satellites that simultaneously solves for global density corrections and individual state vectors for the calibration satellites. DCA uses Space Surveillance Network (SSN) observations directly, thus avoiding any intermediate step of fitting the density correction to time series of estimated ballistic coefficient B_{model} or energy dissipation rate (EDR). This approach also optimizes use of the detailed information contained in the original space surveillance observations. As in MADM, DCA uses the Jacchia 1970 thermosphere as its base model⁵. While MADM corrected only two global temperature parameters of the base model, DCA estimates up to 20 density correction parameters. This global correction not only reduces the errors in the state error covariance for every low perigee satellite, but also makes these errors more realistic. In addition, the sensitivity of orbit accuracy to fit span length is significantly reduced. Once these density correction parameters are computed, they are output to a file so they can be accessed by users to improve orbit determination and prediction for all low

perigee satellites. DCA was developed by Omitron, Inc. in Colorado Springs, Colorado.

An important feature of DCA is its segmented solution approach. Although the state vector of each calibration satellite is solved for a 1.5-day fit span interval, the density correction parameters are solved on 3-hour sub-intervals within the fit span. This approach is used to extract the time resolution needed to accurately estimate the dynamically changing thermospheric density². This is especially important during geomagnetic storms, when the joule heating of the auroral ovals drives rapidly changing density features. The observability of the parameters estimated for each segment is sufficient because of the large number (~75) of calibration satellites used, and because space surveillance tasking was increased to every pass with 10 observations each.

In addition to estimating a density correction, the plan is to also employ a segmented solution for the ballistic coefficient. This is a technique whereby the estimated ballistic coefficient is allowed to vary over the fit span. Fit spans of several days are divided into 1/2 to 3-hour segments for which a separate ballistic coefficient is estimated. The plan is apply the SSB technique after the DCA density corrections are applied, thus further improving the accuracy of the state vector estimate for the satellite trajectory. This technique may only be applied if there is sufficient tracking data to provide the

observability needed for the segmented B . Figures 2 and 3 demonstrate the kind of relative accuracy improvement one can expect from this segmented approach. Figure 2 shows the in-track residuals for a LEO satellite resulting from a 5-day fit. The 5-day fit span and 3-day prediction span are separated by the solid vertical line. Figure 3 shows the same 5-day fit span

after a 6-hour segmented approach is applied. Here, the estimated ballistic coefficient is the parameter whose solution is segmented. We are seeing similar improvements, when instead, we segment the solution of a set of global density correction parameters and hold the estimate for the true ballistic coefficient fixed.

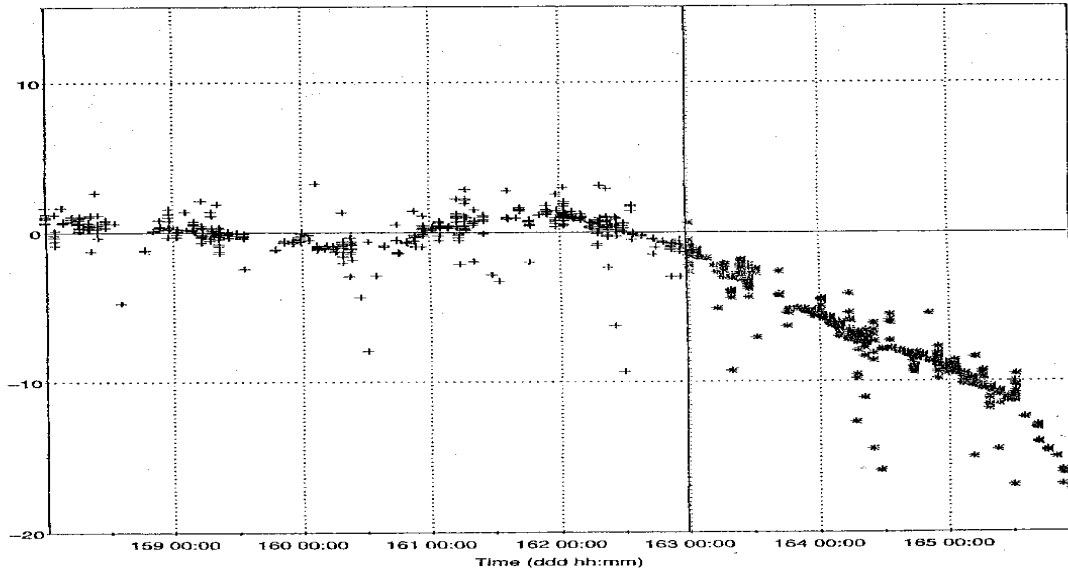


Figure 2. In-Track Residuals for a LEO Satellite (5-Day Fit / 3-Day Prediction)

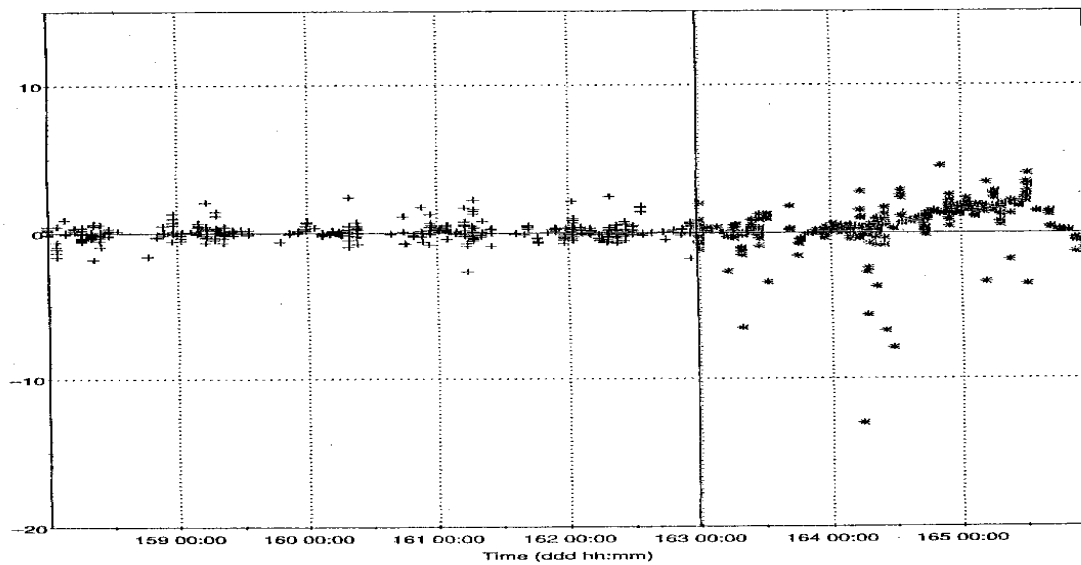


Figure 3. In-Track Residuals for a LEO Satellite (5-Day Segmented Fit / 3-Day Prediction)

Temperature and Density Profiles

For this initiative, 75 calibration satellites are being used simultaneously to solve for a global density correction field. This field corrects two local parameters in the vertical temperature profile leading to a unique density profile; a low altitude parameter and a high altitude parameter). DCA estimates a new set of zeroth degree coefficients for the low-altitude parameter every 3 hours. The other coefficients are estimated every 12 hours. The number of coefficients is given by $(N_{\text{low}} + 1)^2 + (N_{\text{high}} + 1)^2$, where N_{low} and N_{high} are the degree of the spherical harmonic truncation for the low and high parameters respectively. The truncation degrees most successful so far are $N_{\text{low}} = 1$ and $N_{\text{high}} = 2$, for a total of 13 coefficients. After further optimizing this parameter set, the level of truncation may change with a corresponding change in the number of parameters.

The two local temperature parameters (low altitude and high altitude) corrected by DCA are the so-called “inflection point temperature” T_x at 125 km altitude, and the exospheric temperature T_∞ , the asymptotic temperature the profile approaches with increased altitude in the exosphere (>600 km altitude). The local temperature profile $T(z)$ as a function of altitude z is uniquely determined by T_x and T_∞ . The local temperature profile leads to the local density profile through interpolation of density tables, which were produced by integrating the hydrostatic equation (from 90 km to 105 km altitude) and the diffusion equation (above 105 km)⁴.

The local values for T_x and T_∞ are both corrected indirectly through a *global* parameter known as the “nighttime minimum exospheric temperature” T_c . This is the principal parameter used in the standard Jacchia 1970 model to describe the state of the entire thermosphere in response to solar extreme ultraviolet heating⁵, and is given by the following expression:

$$T_c = 383.0 + 3.32F_{10.7} + 1.8(F_{10.7} - \bar{F}_{10.7}) \quad (3)$$

We have also replaced the $F_{10.7}$ index with the new $E_{10.7}$ index, which is based on the true extreme ultraviolet heating of the thermosphere.

In the modified Jacchia 1970 model developed by the AFSPC Space Analysis Center¹⁴, a ΔT_c correction is added to the standard T_c value to produce the corrected value:

$$T'_c = T_c + \Delta T_c \quad (4)$$

The local exospheric temperature T_∞ is obtained from T_c in the same way the standard Jacchia 1970 model obtains T_∞ from T_c ; through multiplying by the diurnal variation factor $D(\delta, \phi, \lambda)$ (a function of solar declination δ , latitude ϕ and local solar time λ), and adding the contribution to T_∞ due to geomagnetic activity ΔT_G and the semi-annual variation ΔT_S . The associated equation is as follows:

$$T'_\infty = T'_c D(\delta, \phi, \lambda) + \Delta T_G(a_p) + \Delta T_S(t, \bar{F}_{10.7}) \quad (5)$$

The local value for T_x is then computed from the local exospheric temperature T'_∞ using the standard Jacchia 1970 expression:

$$T'_x = 444.3807 + 0.02385 T'_\infty - 392.8292 \exp(-0.0021357 T'_\infty) \quad (6)$$

However, in this modified Jacchia model, the local inflection point temperature T_x is further corrected by adding a direct ΔT_x correction to T'_x

$$T''_x = T'_x + \Delta T_x \quad (7)$$

The double prime indicates that this inflection point temperature is corrected twice; once through ΔT_c and again through ΔT_x . Both ΔT_c and ΔT_x are expressed in terms of independent spherical harmonic expansions in latitude and local solar time. Since local solar time is equivalent to the right ascension relative to the anti-solar point, it is better to regard it as an angular coordinate than a time.

When $\Delta T_x = 0$, the temperature profile is identical to a standard Jacchia 1970 profile for a given local exospheric temperature. Figure 4 shows seven temperature profiles, each corresponding to a different local exospheric temperature T'_∞ . These exospheric temperatures vary from 500 to 2000°K, representing the natural range of values. All temperature profiles start from a constant temperature of 183°K at 90 km altitude, the lower boundary. The

temperature increases with altitude, exhibiting an inflection point at a fixed altitude of 125 km, indicated in Figure 4 by the solid black vertical line. The temperature continues to increase and becomes asymptotic to the local exospheric temperature T_∞ . Figure 5 shows seven

temperature profiles, each corresponding to a different T'_x . The inflection point temperatures shown here range from 200°K to 800°K.

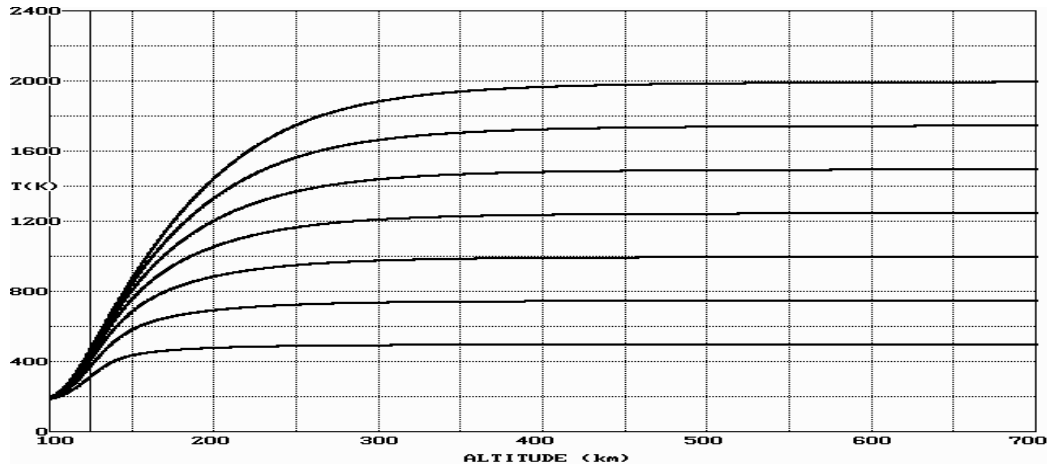


Figure 4. Temperature Profiles ($T_\infty = 500, 750, 1000, 1250, 1500, 1750, 2000^\circ\text{K}$ with $\Delta T_x = 0$)

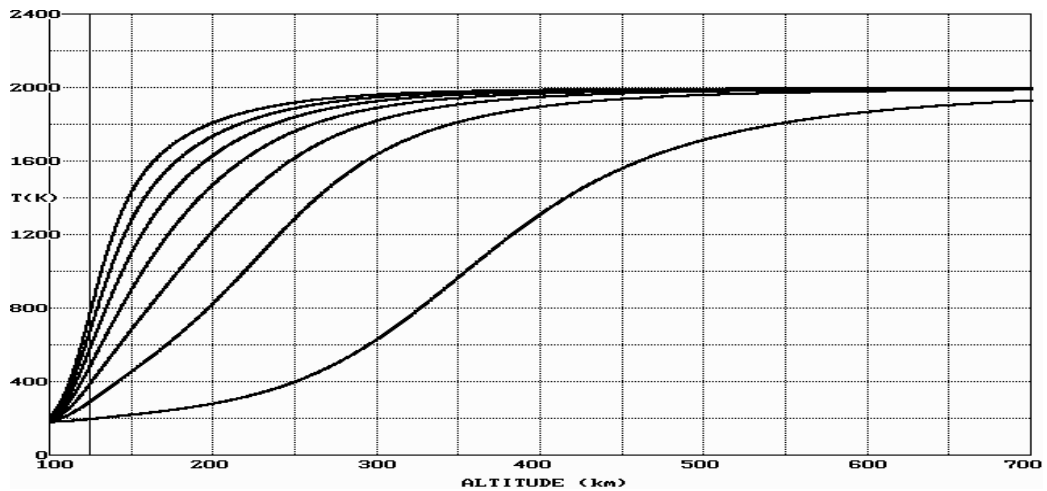


Figure 5. Temperature Profiles ($T'_x = 200, 300, 400, 500, 600, 700, 800^\circ\text{K}$ with $T_\infty = 2000^\circ\text{K}$)

These T'_x values occur along the solid black vertical line at an altitude of 125 km. To explore the effect of changing T'_x only, the exospheric temperature in Figure 5 was held constant at $T_\infty = 2000^\circ\text{K}$. Changing T'_x acts to flatten ($\Delta T_x < 0$) or steepen ($\Delta T_x > 0$) the temperature gradient with altitude. For T'_x values less than $\sim 400^\circ\text{K}$, a second inflection point appears at altitudes above 125 km. As T'_x decreases, this second inflection point dominates the one at 125 km.

The local density profile is computed from the local temperature profile by integrating the hydrostatic and diffusion equations subject to the lower boundary conditions at 90 km altitude. Figure 6 displays neutral density as a function of altitude and T_∞ . Figure 7 displays neutral density as a function of altitude and T'_x . The key to understanding the relationship between the density profiles and the temperature profiles is to recognize that the thickness of a particular density interval (color band) measured along a

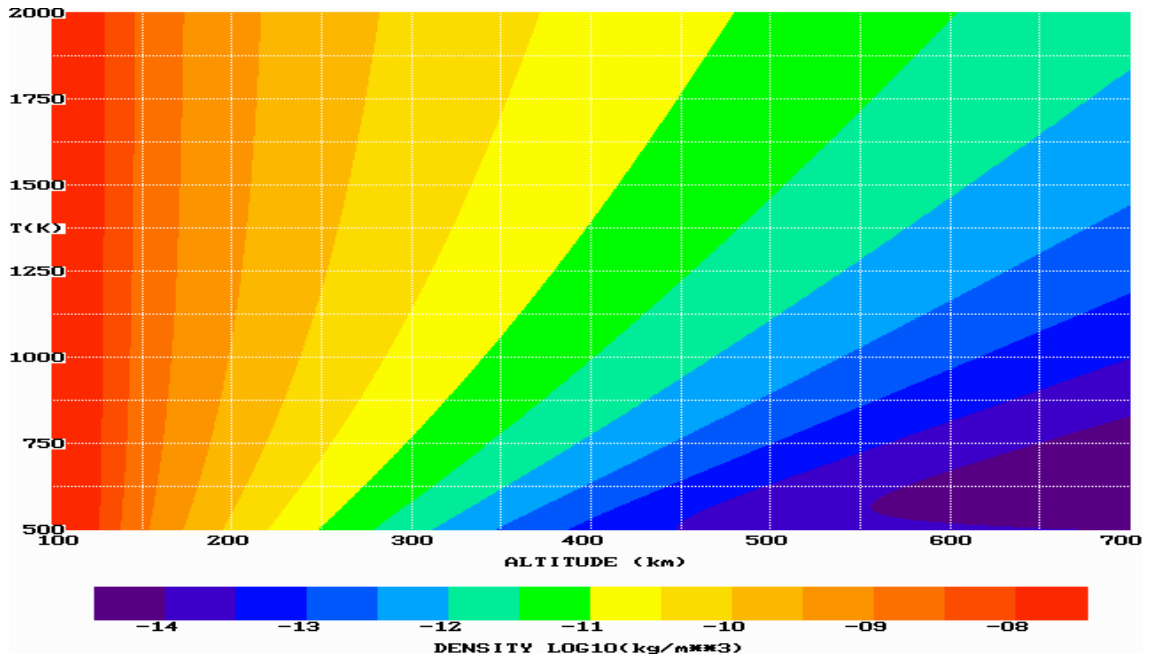


Figure 6. Density versus Altitude and Exospheric Temperature T_∞ (with $\Delta T_x = 0$)

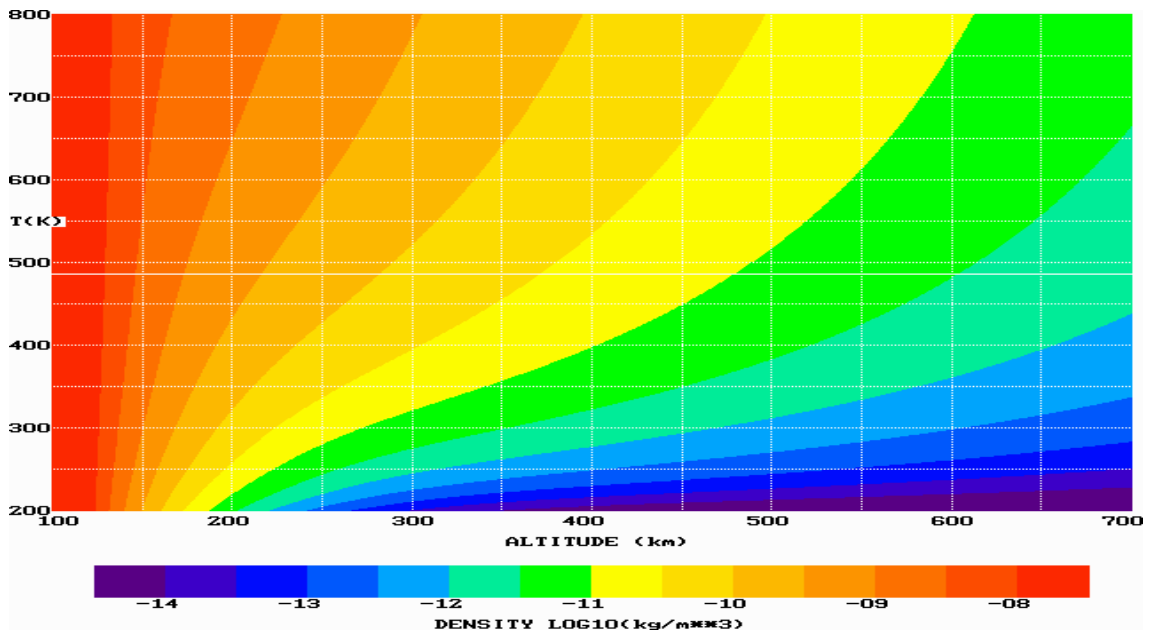


Figure 7. Density versus Altitude and Inflection Temperature T'_x (with $T_\infty = 2000^\circ\text{K}$)

horizontal (constant temperature) line, is proportional to the scale height⁶. Although the scale height is dependent on several things (temperature, mean molecular weight, diffusion coefficient and gravity acceleration), it is strongly proportional to the local temperature at a given altitude. Therefore, to a first approximation, the vertical density gradient is inversely proportional to the local temperature. Note in Figure 6 (standard profiles) that the scale heights increase with altitude throughout the thermosphere, above which they are nearly constant. This happens at higher altitudes for higher exospheric temperatures. In Figure 7 it can be seen that the local inflection point temperature T'_x affects the density profile by raising ($\Delta T_x < 0$) or lowering ($\Delta T_x > 0$) the altitude range where the scale heights change most rapidly. The horizontal solid white line indicates the standard value ($T'_x = 487^\circ\text{K}$) when $\Delta T_x = 0$ for an exospheric temperature of $T_\infty = 2000^\circ\text{K}$. Above ~ 250 km altitude, changing T'_x has an effect similar to multiplying the model density by a constant factor, or equivalently, shifting $\log_{10}(\rho)$ by a constant without significantly affecting the scale height. On the other hand, changing T_∞ alters the scale height as well as the density at all altitudes. Allowing T'_x to deviate from the standard Jacchia 1970 value affords an additional degree of freedom for estimating the density profile, resulting in a better fit to the true density.

Density Prediction Technique

We make use of the 3-day prediction of a_p as well as a 3-day prediction of $E_{10.7}$, produced by the SOLAR2000 solar irradiance model. This model was developed by Space Environment Technologies, Inc. for the Space Environment Center and other agencies¹⁵. SOLAR2000 is the first- ever empirical full solar spectrum model. Its spectral resolution is 1 nm and extends from X-rays through the infrared (IR) spectrum. The temporal resolution extends from minutes to a full solar cycle (~ 11 years). It acts like a data fusion engine and ingests data from ultraviolet (UV) and extreme ultraviolet (EUV) sensors, ground-based optical sensors and total irradiance sensors and imagers. For the High Accuracy Satellite Drag Model, we are using the SOLAR2000's index, as well as the classic $F_{10.7}$ index. $E_{10.7}$ is based on the total solar irradiance integrated over all relevant EUV wavelengths

and is integrated in time over the past 24 hours. The resulting EUV flux was plotted versus the simultaneous $F_{10.7}$ indices and a curve was fit to the points. This curve was then used to translate the integrated EUV flux to the $E_{10.7}$ index. A similar procedure is being used to generate an $E_{10.7}$ corresponding to the 81-day centered mean of the $F_{10.7}$ index. When $E_{10.7}$ is used instead of $F_{10.7}$, it automatically increases the accuracy of the thermospheric density model, even if that model was constructed using the $F_{10.7}$ index. Currently, SOLAR2000 produces a now-cast and 3-day prediction of the $E_{10.7}$ index.

The density correction coefficients from the Dynamic Calibration Atmosphere (DCA) are predicted out 3 days into the future using a prediction filter that relates the $E_{10.7}$ time series and the geomagnetic index a_p time series to these coefficients, as well as extrapolation of the past time series of the coefficients themselves¹⁶. All of the DCA coefficients are expressed as a separate function of the time series of their past values, as well as the predicted indices ($E_{10.7}$ and a_p). This density prediction filter extrapolates the recent (last ~ 27 days) behavior of the time series of the DCA density correction coefficients. The behavior is deduced through Fourier analysis of the frequency, phase, and amplitude of the coefficients. The behavior of the coefficient time series is tied to the solar/geomagnetic heating indices. Therefore, the extrapolated time series is adjusted according to the values of the predicted indices. In this way, we can leverage off the existing space forecast expertise in predicting the indices. This prediction filter should significantly boost the prediction accuracy of the existing thermospheric model in response to predicted indices. Space Environment Technologies, Inc. is finalizing this prediction filter.

Laboratory Assistance

Both Air Force Research Laboratory (AFRL) and Naval Research Laboratory (NRL) are participating in this project. Air Force Research Laboratory is validating the new $E_{10.7}$ index over one solar cycle. AFRL is also validating the density prediction technique developed by Space Environment Technologies, Inc. This is being accomplished by comparing the spherical harmonic coefficients produced by the prediction

filter to the actual coefficients estimated by DCA.

Naval Research Laboratory is comparing the density field estimated by DCA to the density field produced by their MSIS2000 model^{4,12}. This model is designed to ingest data from the Special Sensor Ultraviolet Limb Imager (SSULI). This is a space-based airglow sensor that measures ultraviolet emissions from the thermosphere and ionosphere to deduce densities of individual neutral and ion gas species. The MSIS2000 model is then adjusted to these measurements, thus producing total neutral density. Any discrepancies between DCA and MSIS2000 will be analyzed and the models will be adjusted as appropriate. This will pave the way for a possible thermospheric density data fusion effort. Such fusion of real-time data will be indispensable for the initialization of physics-based thermospheric density models, ionospheric models, and combined thermosphere/ionosphere models.

Conclusion

Atmospheric density models for computing drag forces on satellites are a major source of inaccuracy in trajectory predictions for low-perigee satellites. This deficiency can result in serious errors in the predicted position of satellites, especially those orbiting below 600 km altitude, the layer known as the thermosphere. Many of these objects are of high interest to Space Control missions.

Current thermospheric density models do not adequately account for dynamic changes in atmospheric drag for orbit predictions, and no significant operational improvements have been made since 1970. Lack of progress is largely due to poor model inputs in the form of crude heating indices, as well as poor model resolution, both spatial and temporal. The High Accuracy Satellite Drag Model (HASDM) initiative uses the Dynamic Calibration Atmosphere (DCA) algorithm to solve for the thermospheric density near real-time from the “observed” drag effects on a set of low-perigee inactive payloads and debris (*calibration satellites*). Many different calibration satellites with different orbits may be exploited to recover an accurate global density field. The greater the number of calibration satellites, the better the accuracy. For this initiative, we are using 75 such satellites.

There are four major innovations within this initiative that should improve the way satellite drag is determined and predicted:

- **Dynamic Calibration Atmosphere (DCA)**
This algorithm determines an accurate global density correction from which we can model the true density to within a few percent. It estimates this density correction every 3 to 12 hours.
- **New EUV Index ($E_{10.7}$)** This index is generated by the new SOLAR2000 model, the first full spectrum model of solar electromagnetic radiation. Not only does this index better represent the true heating of the thermosphere due to solar extreme ultraviolet (EUV) radiation, but also can be more accurately predicted out 3 days or more.
- **Prediction Filter for DCA Corrections**
This density prediction filter extrapolates the recent (last ~27 days) behavior of the time series of the DCA density correction coefficients. The behavior is deduced through Fourier analysis of the frequency, phase, and amplitude of the coefficients. The extrapolated time series is adjusted according to the values of the predicted solar and geomagnetic indices.
- **Segmented Solution for Ballistic Coefficient (SSB)** This is a technique whereby the estimated ballistic coefficient is allowed to vary over the fit span. Fit spans of several days are divided into ½ to 3-hour segments for which a separate ballistic coefficient is estimated. The plan is apply the SSB technique after the DCA density corrections are applied, thus further improving the accuracy of the state vector estimate for the satellite trajectory.

A fair amount of success has come from previous efforts using spherically symmetric density corrections^{10,11}. However, this horizontally and temporally varying correction produces a significantly more accurate density solution. The estimated spherical harmonic coefficients may be readily used to specify and predict a corrected global density field which can be applied to special perturbations orbit determination and prediction for any low-perigee satellite. Accuracy requirements for all Space Control missions should be met at a much better rate. This initiative could also provide an accurate neutral density database for basic research.

Acknowledgment

We would like to thank our colleagues, Mr. Robert Morris and Dr. Joseph Liu, as well as Mr. William Barker and Mr. Steve Casali of Omitron Inc. and Dr. Kent Tobiska of Space Environment Technologies, Inc. for their valuable contributions and insight. We also thank Mr. Frank Marcos of Air Force Research Laboratory for his valuable suggestions and guidance.

References

1. Bowman, Bruce R.; "True Satellite Ballistic Coefficient Determination for HASDM," AIAA-2002-4887, *AIAA/AAS Astrodynamics Specialist Conference* (Monterey, California), Aug 2002.
2. Casali, Stephen J. and Barker, William N.; "Dynamic Calibration Atmosphere (DCA) for the High Accuracy Satellite Drag Model (HASDM)," AIAA-2002-4888, *AIAA/AAS Astrodynamics Specialist Conference* (Monterey, California), Aug 2002.
3. Hedin, A. E.; Spencer, N. W. and Mayr, H. G.; "The Semidiurnal and Terdiurnal Tides in the Equatorial Thermosphere from AE-E Measurements," *J. Geophys. Res.*, **85**, pp. 1787-1791, 1980.
4. Hedin, A. E.; "Extension of the MSIS Thermosphere Model into the Middle and Lower Atmosphere," *J. Geophys. Res.*, **96**, pp. 1159-1172, 1991.
5. Jacchia, L. G.; "New Static Models of the Thermosphere and Exosphere with Empirical Temperature Profiles", Smithsonian Astrophysical Observatory (Special Report 313), May 1970.
6. Jursa, Adolph S., ed.; *Handbook of Geophysics and the Space Environment*, Air Force Geophysics Laboratory (USAF), 1985.
7. Liu, Joseph J. F.; "Advances in Orbit Theory for an Artificial Satellite with Drag", *Journal of Astronautical Sciences*, **XXXI**, No. 2, pp. 165-188, April-June 1983.
8. Liu, Joseph J. F., France, R. G. and Wackernagel, H. B.; "An Analysis of the Use of Empirical Atmospheric Density Models in Orbital Mechanics", *AAS/AIAA Astrodynamics Specialist Conference* (Lake Placid, New York), August 1983.
9. Marcos, Frank A.; "Accuracy of Atmosphere Drag Models at Low Satellite Altitudes," *Adv. Space Research*, **10**, (3) pp. 417-422, 1990.
10. Marcos, Frank A.; Kendra, M. J.; Griffin, J. M.; Bass, J. N.; Liu, J. J. F. and Larson, D. R.; "Precision Low Earth Orbit Determination Using Atmospheric Density Calibration," *Advances in Astronautical Sciences*, **97** (1), pp. 515-527, AAS, 1998.
11. Nazarenko, Andrey I.; Cefola, P. J. and Yurasov, V.; "Estimating Atmospheric Density Variations to Improve LEO Orbit Prediction Accuracy," AAS 98-190, *AAS/AIAA Space Flight Mechanics Meeting* (Monterey, CA), February 1998.
12. Nicholas, A. C.; Picone, J. M. and Thonnard, S. E.; "Methodology for Using Optimal MSIS Parameters Retrieved from SSULI Data to Compute Satellite Drag on LEO Objects", *AAS/AIAA Astrodynamics Specialist Conference* (Girdwood, Alaska), August 1999.
13. Snow, Daniel E. and Liu, Joseph J. F.; "Atmospheric Variations Observed from Orbit Determination", *AAS/AIAA Astrodynamics Specialist Conference* (Durango, Colorado), August 1991.
14. Storz, Mark F.; "Satellite Drag Accuracy Improvements Estimated from Orbital Energy Dissipation Rates", *AAS/AIAA Astrodynamics Specialist Conference* (Girdwood, Alaska), August 1999.
15. Tobiska, W. Kent; Woods, Tom; Eparvier, Frank; Viereck, Rodney; Floyd, Linton; Bouwer, Dave; Rottman, Gary and White, O. R.; "The SOLAR2000 Empirical Solar Irradiance Model and Forecast Tool", *Journ. of Atmos. and Solar-Terrestrial Physics*, April 2000.
16. Tobiska, W. Kent; "E_{10.7} Use for Global Atmospheric Density Forecasting in 2001," AIAA-2002-4892, *AIAA/AAS Astrodynamics Specialist Conference* (Monterey California), Aug 2002.